Chapter 4

Role of Linear Polyacene Spacers in Intramolecular Magnetic Exchange Coupling

The estimation of intramolecular exchange coupling constant (J) for 10 different oxo- and thioxo-verdazyl based high spin ground state diradicals with linear polyacene couplers of varying length using the broken symmetry approach in an unrestricted DFT framework is described in this chapter. The magnetic characteristics of these systems are explained using the spin-density distribution, and an analysis is made by "magnetic" orbitals. The Nuclear Independent Chemical Shift (NICS) values have been calculated for these diradicals. The average NICS(1) (1Å above the ring surface) value per benzenoid ring increases as the size of the coupler increases. So-called ΔNICS(1) values [the difference among average NICS(1) per benzenoid ring in the coupler and the NICS(1) of the linear polyacene molecule] are correlated with J values. Bond orders and hyperfine coupling constant values have also been evaluated and analyzed for these diradicals.

4.1. Introduction

In the last few decades, experimentalists as well as theoreticians have paid special attention to the design, characterization and application of ferromagnetic materials based on organic diradicals.[1-3] The first purely organic magnetic material, based on the β-crystal phase of *p*-nitrophenyl nitronyl nitroxide radical, was discovered by Kinoshita and co-workers,[4] and has thrust the work nearer to the target of an organic ferromagnet. It is often important to have proper apprehension about the intramolecular magnetic exchange coupling constants before synthesizing organic diradicals intended as prospective ferromagnets.[1] As the aromatic linear fused-ring couplers of varying length can be synthesized easily, an interest has grown up concerning diradicals coupled with polyacene spacers.

Only a few organic paramagnetic species have reasonable stability to be suitable for the design of organic molecular ferromagnets.[5,6] Organic radicals such as nitronyl nitroxide, verdazyl, tetrathiafulvalene are appropriate for this purpose. The advantage of working with such systems is that they do not have any bulky substituent.[7] Nitronyl nitroxide diradical with ethylene coupler, isolated and studied by Ziessel et al.,[8] shows a very high exchange coupling constant. In the DFT framework, Ali and Datta[9,10] have comprehensively studied nitronyl-nitroxide-based molecular ferromagnets with different π-conjugated couplers. The potentiality of verdazyl radical as a precursor of molecular magnets remained unnoticed for a long time,[11,12] although it was first synthesized by Kuhn and Trischmann.[13] The spin-active verdazyl moiety is a good option for the design of molecular magnets. Non-Kekulé bis-oxoverdazyl diradical remains in the singlet ground state with small amount of thermally populated "triplet".[14] Brook et al.[15] have also extensively studied its electronic properties and found that it is strongly antiferromagnetically coupled. The HOMO and LUMO of bis-oxoverdazyl diradicals are similar to those of tetramethylene ethane (TME).[15,16] Substitution of both of the oxygen atoms in bis-oxoverdazyl diradical by sulfur atoms (bis-thioxoverdazyl diradical) gives a red shift.[17] Fico et al.[14] have reported that the room-temperature EPR spectrum of bis-thioxoverdazyl diradical is similar to that of the bis-oxoverdazyl diradical. They also have found that there is a notable variation in electron density between the oxo and thioxo derivatives. The magnetic properties of different derivatives of verdazyl radicals have

been studied extensively.[11,12,18-26] The radicals, 6-oxo- and 6-thioxo-verdazyl are also known to be chemically stable. They can be isolated in solvent-free pure forms in the crystalline state.[17,27] Azidophenyl substituted verdazyls have also been prepared by Lathi and co-workers.[28] Hicks et al.[29] have studied the supra-molecular chemistry of verdazyl molecules. Phosphaverdazyl radicals are also synthesized and characterized by Hicks and Hooper.[30]

The intramolecular magnetic exchange-coupling constant (J) as described by Heisenberg Hamiltonian is the best known descriptor of magnetism. The value of J depends on the molecular geometry of the diradicals and the unpaired-electron structures. Prior knowledge of the magnetic exchange-coupling constant characteristics becomes useful before synthesizing molecular ferromagnets.[1] In a diradical, the exchange-coupling constant depends crucially on the distance between two radical centers and the nature of the couplers. Gilroy et al.[31] have synthesized various verdazyl based compounds and characterized their magnetic properties. Applying unrestricted density functional methodology, intramolecular magnetic exchange-coupling constants have been studied for a series of bis-nitronyl nitroxide diradicals bridged with different π-couplers by Ali and Datta.[9] Polo et al.[32] have investigated tetrathiafulvalene (TTF) and verdazyl diradical cations with similar couplers. Although, in that work they have criticized the use of spin projected techniques and decided not to use it, but they finally end up using one such method. In a recent work, Latif et al.[33] investigated polyene spacers with mixed radical systems, in which they have established that the magnitude of the coupling constant depends strongly on the planarity of the molecular structure, spin polarization paths, length of the couplers, etc. In some recent work, we have designed and investigated 11 bis-oxoverdazyl diradicals connected by different linkage-specific aromatic couplers and found that *meta*-coupled diradicals are ferromagnetic whereas *para*-coupled diradicals are antiferromagnetic in nature.[34] Logically, our present chapter follows these investigations, where the objective is to design and characterize oxoverdazyl and thioxoverdazyl based molecular ferromagnets coupled with different polyacene spacers. We have designed two sets of diradicals, (set A with 5 bis-oxoverdazyl diradicals and set B with 5 bis-thioxoverdazyl diradicals) coupled by different *meta*-connected linear polyacene

Scheme 4.1. General schematic representation of diradicals (i-x) with five different polyacene couplers, where formally there are two unpaired electrons at N_4 and N_{10} atoms and the benzenoid rings are denoted as A, B, C, D and E . The polyacene couplers (X=1 to 5) are used in both sets of diradicals.

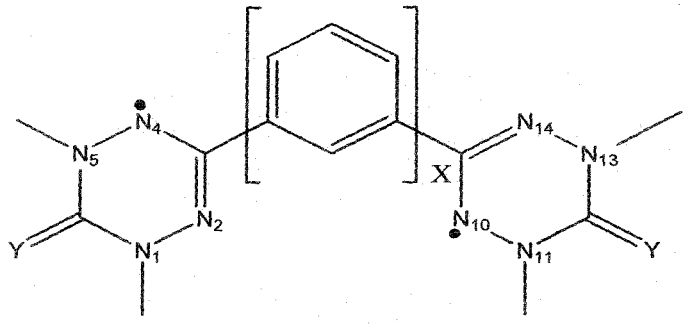

where Y=O (Set A) and S (Set B) and X=1-5

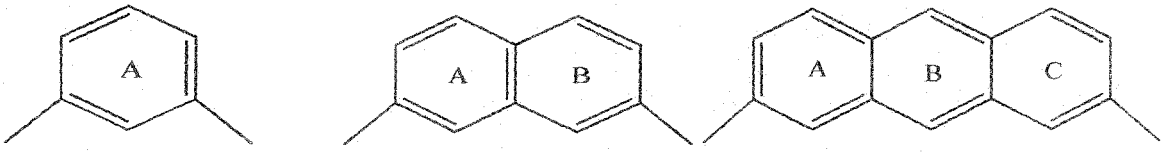

Diradical (i), X=1, Y=O Diradical (ii), X=2, Y=O Diradical (iii), X=3, Y=O

Diradical (vi), X=1, Y=S Diradical (vii), X=2, Y=S Diradical (viii), X=3, Y=S

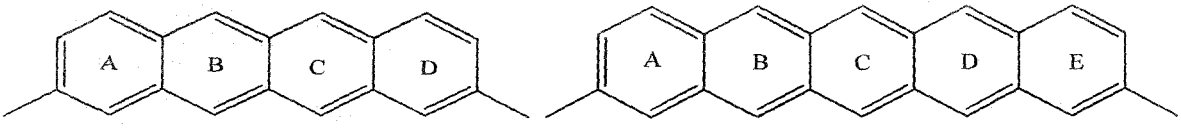

Diradical (iv), X=4, Y=O Diradical (v), X=5, Y=O

Diradical (ix), X=4, Y=S Diradical (x), X=5, Y=S

spacers of varying length. The designed systems are depicted in Scheme 4.1. Some of the systems under investigation are already synthesized and characterized.[14,31] It is noticed that the magnetic exchange coupling constant depends on the length of the coupler and spin polarization path. The polyacenes are aromatic hydrocarbons with linearly fused benzene rings.[35] Experimentalists as well as theoreticians have been attracted by these substances for a long time.[36] Pentacenes are known to have semiconducting property[35,37] hence; it can be used in spintronic materials. It is established that the polyacenes are predicted to have smaller band gaps than the corresponding polyenes.[38] The polyacenes become less stable with increasing numbers of benzene rings.[35,36] In this chapter, we find, linear polyacene coupled bis-oxo- and bis-thioxo-verdazyl diradicals have moderate ferromagnetically signed exchange-coupling constants. The exchange coupling constants are evaluated through the spin-polarized unrestricted DFT methodology. The broken-symmetry (BS) approach, described in the next section, has been adopted here to quantify ferromagnetic coupling constants for all the systems described above.

4.2. Theoretical Background and Computational Details

The Heisenberg spin Hamiltonian is normally used to express the magnetic exchange interaction between two magnetic sites 1 and 2,

$$\hat{H} = -2J\hat{S}_1 \bullet \hat{S}_2, \tag{4.1}$$

where J is the exchange coupling constant between two magnetic centers of a diradical, with $\hat{S}_1$ and $\hat{S}_2$ being the respective spin angular momentum operators. The square of the total spin operator $\hat{S}^2$ has eigenvalue $S(S+1)$. A positive sign of J, in which a situation of parallel spin is essential, is used to indicate a ferromagnetically signed interaction, whereas an antiferromagnetically signed interaction is indicated by a negative value, where a state of antiparallel spins is favored. For a diradical with a single unpaired electron on each site, J can be written as

$$E_{(S=1)} - E_{(S=0)} = -2J. \tag{4.2}$$

A single determinantal wave function in the unrestricted Hartree Fock formalism cannot truly represent the singlet state of a diradical. Moreover, this introduces spin contamination in such calculations. Therefore, this method cannot directly yield reliable J values. However, one can evaluate J by determining the exact singlet and "triplet" energy values from a multiconfigurational approach and MCSCF calculations on bis-verdazyl systems have been carried out.[39] The performance of the complete active space second-order perturbation theory (CASPT2) and accurate Difference Dedicated Configuration Interaction (DDCI) calculations for α-4-dehydrotoluene and 1,1',5,5'-tetramethyl-6,6'-dioxo-3,3'-bis-verdazyl and other diradicals have also been reported by Illas and coworkers[40] and the authors found that CASPT2 provides a clean alternatives to the use of BS-UDFT based methods. However, these methods are resource intensive and are not employed in this chapter. On the other hand, the broken-symmetry (BS) formalism proposed by Noodleman[41,42] in a DFT framework is an alternative approach to evaluate J with less computational effort. The BS state, which is a weighted average of low- and high-spin states, is often found to be spin contaminated. But with the use of a "spin-projection" technique, reliable estimates of the exchange-coupling constant can be obtained via this BS approach. Depending upon the extent of overlap between magnetic orbitals, different expressions for J have been proposed by many researchers,[40-57] using the unrestricted spin-polarized BS solution for the lower-spin state. The expression for J given by Ginsberg,[43] Noodleman,[44] and Davidson[45] is more useful when overlap of the magnetic orbitals is very small. The expression put forward by Bencini and coworkers,[46,47] Ruiz et al.[48] uses the energy of the BS state as that of the open-shell singlet without spin projection and attempt to justify their choice (later on) by the hypothesis of the large overlap limit between magnetic orbitals. However, this approach has been shown to be unphysical by Caballol et al.,[50] where the overlap is explicitly calculated and found to be small. In a more recent work, Moreria and Illas[52] have shown that there exists a common physical background in the magnetic interactions in organic diradicals, inorganic complexes or ionic solids, where the magnetic interactions occur between localized spins. Further, Illas and coworkers[51-53] have shown that Spin Unrestricted Broken Symmetry (SUBS) and Spin-Restricted-Ensemble-referenced Kohn-Sham (REKS) lead to similar estimate of J value. However, exchange correlation

functional used in REKS approach is under development and performance of each functional is yet to be explored.

Nevertheless, in this chapter, the Yamaguchi model[54-57] is employed to get the J values, and this is the proper choice, especially if one is uncertain of the magnitude of J beforehand. The expression is

$$J = \frac{(E_{BS} - E_T)}{\langle S^2 \rangle_T - \langle S^2 \rangle_{BS}}, \tag{4.3}$$

where E_{BS} and E_T denote the energy of the broken symmetry singlet and "triplet" state, and where $\langle S^2 \rangle_T$ and $\langle S^2 \rangle_{BS}$ represent respective average spin-square values in "triplet" and BS states. It should be noted here that E_T is the approximate form of $E_{T'}$, the energy of the "triplet" state in the unrestricted formalism using the BS orbital. The approximation is valid because of the very less spin contamination in the high spin state.[9,10] However, even for this high symmetry states the spin unrestricted calculations converge to a state which has not spin well defined. As $\langle S^2 \rangle_T$ is near 2 and $\langle S^2 \rangle_{BS}$ is near 1, eq (4.3) reduces essentially to the case with small overlap and the denominator is just a very small correction.

The energy differences in B3LYP calculations are accurate to ± 2-5 kcal/mole. In this chapter, the computed energy difference is less than 0.1 kcal/mole. As a result, this is not surprising that the J values may be little overestimated. Nevertheless, in this chapter we get the sign of exchange coupling right and therefore correctly predict the nature of coupling. Ruiz et al. [58] related the overestimation of J values with the presence of high self interaction error (SIE) in commonly used DFT exchange correlation potentials. However, this has been severely questioned by a comment co-authored by a large list of specialists in this field.[59] Polo and coworkers[60] have concluded that the presence of SIE in commonly used DFT approximations is related to "nondynamic" correlation energy. Hybrid functionals are more suitable than pure DFT functionals in BS-UDFT calculations because the former reduces the self interaction error (SIE) of DFT exchange functionals.[61] The suitability of B3LYP over LSDA and GGA approach has also been justified by Martin and Illas.[62] Thus, one can

surmise that as B3LYP functional is parameterized mainly to molecules composed of light atoms, it likely to give superior energy differences in such molecules. In this chapter, the molecular geometries of a sequence of compounds (i-x) have been fully optimized with the UB3LYP[63-65] exchange correlation potential using a 6-31G(d,p) basis set.[66-68] At the optimized geometries energy calculations of each of the species are then done with a larger basis set i.e., 6-311++G(d,p), and these are used to calculate the *J* values. To obtain the open-shell BS singlet solution, "guess =mix" keyword is used within the unrestricted formalism. The BS states are stable for all 10 diradicals. All the calculations have been carried out using the GAUSSIAN 03W[69] quantum chemical package. Hyperchem 7.5[70] and Molekel 4.0[71] softwares have also been used for visualization. All computations of this chapter have been carried out in a HP xw4600 workstation, processor Intel® Core (TM) 2 Duo CPU @ 2.33 GHz, 3,072 MB of RAM with 64-bit operating system.

4.3. Results and Discussion

The main characteristic of the radicals of the verdazyl family is their stability as well as their ferromagnetic nature in suitably designed diradicals.[40,72] The optimized structures of the systems under investigation are planar (Figure 4.1). As a result, better spin polarization along the π-conjugated network stabilizes the "triplet" states.[73,74] The linker between two same or different organic radicals plays a major role in determining the sign and magnitude of exchange coupling constants.[9,10,32-34] We examine spin coupling between radical centers separated by polyaromatics, using density functional theory to calculate values of the exchange coupling constants (Table 4.1) from the differences in high-spin and low-spin broken symmetry energies for two sets (set A and set B) of compounds, some of which are already known,[14,31] and the others are newly designed as given in Scheme 4.1 (also see Figure 4.1). In set A, we have considered *meta*-coupled diradicals with general formula OV-*X*-OV, where X [when *X*=1 (benzene coupler), 2 (naphthalene coupler), 3 (anthracene coupler), 4 (tetracene coupler), 5 (pentacene coupler)] is the number of aceneic benzene ring(s) used as couplers and OV is oxo-verdazyl monoradical, whereas for set B diradicals, –OV radicals are replaced by –TV (thioxo-verdazyl) radicals. It is established that the unpaired spins are equally distributed among the specified atoms of the diradicals (N_2, N_4,

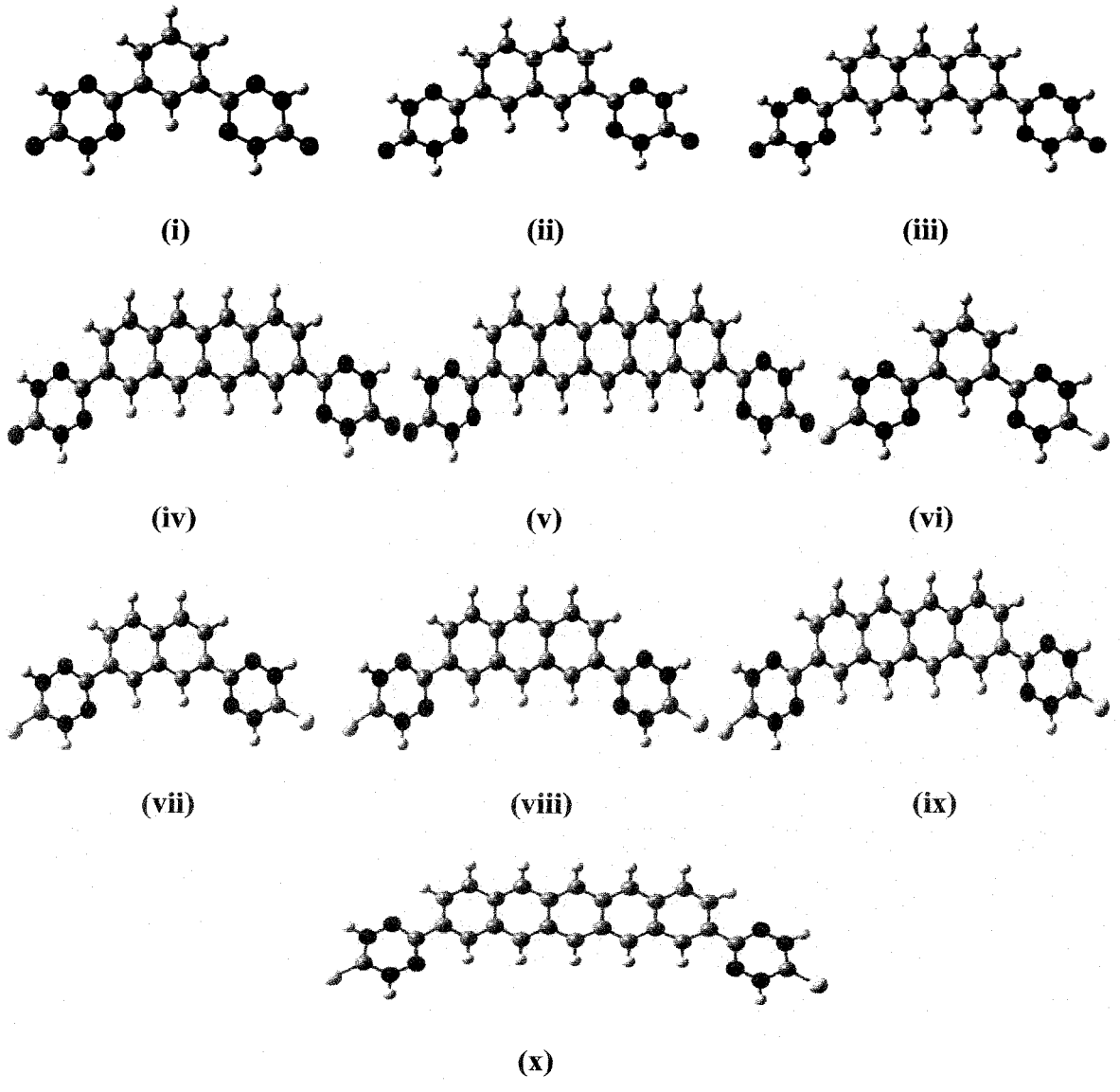

Figure 4.1. The optimized images of polyacene coupled bis-oxoverdazyl (i-v) and bis-thioxoverdazyl (vi-x) diradical systems at UB3LYP/6-31G(d,p) level. Atoms having red, blue, black, yellow and white colors represent O, N, C, S, and H, respectively.

N_{10} and N_{14} in Scheme 4.1).[7] Numerical values of J are obtained by use of eq (4.3) for all 10 species, and are reported in Table 4.1. Normally, the sign of J does not depend on the basis set employed;[32] hence the nature of predicted magnetic behavior in this chapter is reliable. Through close inspection of Table 4.1, it can be inferred that consistent results have been obtained with different basis sets and all 10 diradicals are ferromagnetic in nature. The methyl groups linked with verdazyl N atoms are replaced by hydrogen atoms to save the

Table 4.1. UB3LYP level absolute energies in *au*, $\langle S^2 \rangle$ and intramolecular exchange-coupling constant (J cm^{-1}) using 6-31G(d,p) and 6-311++G(d,p) basis sets, for bis-oxoverdazyl diradicals (i-v) and bis-thioxoverdazyl diradicals (vi-x).

		At UB3LYP/6-31G(d,p) level			At UB3LYP/6-311++G(d,p) level		
Di radicals		BS	"Triplet"	J(cm^{-1})	BS	"Triplet"	J(cm^{-1})
(i)	E	–974.25460	–974.25491	67	–974.50782	–974.50816	74
	$\langle S^2 \rangle$	1.049	2.059		1.048	2.055	
(ii)	E	–1127.90269	–1127.90284	33	–1128.18659	–1128.18673	31
	$\langle S^2 \rangle$	1.050	2.060		1.052	2.056	
(iii)	E	–1281.54431	–1281.54432	02	–1281.85856	–1281.85858	04
	$\langle S^2 \rangle$	1.056	2.065		1.052	2.054	
(iv)	E	–1435.18313	–1435.18315	04	–1435.52783	–1435.52801	39
	$\langle S^2 \rangle$	1.058	2.078		1.052	2.057	
(v)	E	–1588.82059	–1588.82080	44	–1589.19595	–1589.19614	41
	$\langle S^2 \rangle$	1.079	2.138		1.059	2.068	
(vi)	E	–1620.17104	–1620.17131	59	–1620.42061	–1620.42081	44
	$\langle S^2 \rangle$	1.047	2.054		1.047	2.051	
(vii)	E	–1773.81940	–1773.81944	09	–1774.09948	–1774.09965	37
	$\langle S^2 \rangle$	1.049	2.055		1.048	2.053	
(viii)	E	–1927.46107	–1927.46110	07	–1927.77164	–1927.77178	31
	$\langle S^2 \rangle$	1.050	2.060		1.048	2.053	
(ix)	E	–2081.09999	–2081.10004	11	–2081.44114	–2081.44120	13
	$\langle S^2 \rangle$	1.054	2.072		1.051	2.054	
(x)	E	–2234.73756	–2234.73776	42	–2235.10927	–2235.10941	31
	$\langle S^2 \rangle$	1.072	2.128		1.055	2.061	

computation time.[32] In other recent work,[34] the bis-oxoverdazyl diradical with no coupler has been found to generate a strong antiferromagnetically signed interaction according to DFT computations, as is in good agreement with previous experimental studies.[15] In this chapter, we find that the *meta*-aceneic coupled bis-oxoverdazyl and bis-thioxoverdazyl diradicals manifest a ferromagnetically signed interaction, which is also in good agreement with other works.[9,10,31,34] The decreasing order of calculated J values from (i)-(iii) in set A and (vi)-(viii) in set B are also in good agreement with the work of Ali and Datta.[10] The change in J values from (iii)-(v) in set A and (viii)-(x) in set B can be attributed to the fact that the larger polyacenes possess open-shell singlet ground states.[35] However, with our larger basis set, the J value obtained for diradical (viii) is marginally higher than expected.

4.3.1. Bond Order

Using natural bond-order (NBO) analysis we have calculated the Wiberg bond order[75] at the UB3LYP/6-31G(d,p) level. The calculated average Wiberg bond orders between the

Table 4.2. The calculated average Wiberg bond order for the linkage bond between the monoradical and the coupler on both sides, for all the diradicals (i-x) at the UB3LYP level using a 6-31G(d, p) basis set.

Diradicals	Wiberg bond order
(i)	1.042
(ii)	1.045
(iii)	1.048
(iv)	1.050
(v)	1.051
(vi)	1.048
(vii)	1.053
(viii)	1.056
(ix)	1.059
(x)	1.061

coupler and the monoradical moieties on both sides for each of the 10 diradicals are given in Table 4.2. With the increase in the number of benzenoid rings in the coupler, the number of delocalizable π-electrons increases and small increment in Wiberg bond order is noted. It can also be observed that as the average bond order increases, the average Mulliken atomic spin densities decrease modestly on the radical centers (Table 4.3) for the first three diradicals of each set. As a consequence, the magnitude of J value also decreases for the first three diradicals in both sets. On the other hand, for the last two diradicals in every set, with the increase of the diradical character of the coupler, the average Mulliken atomic spin density on the radical centers increases and hence the J value.[10]

Table 4.3. The calculated Mulliken atomic spin densities for all the diradicals (i-x) with the couplers at UB3LYP level using 6-31G(d,p) basis set [N_2, N_4 and N_{10}, N_{14} (Scheme 4.1) are the respective atoms in the verdazyl moiety where the unpaired spins are delocalized (Ref. 7)].

Diradicals	N_2	N_4	Average	N_{10}	N_{14}	Average
(i)	0.4307	0.4326	0.4317	0.4318	0.4316	0.4317
(ii)	0.4435	0.4191	0.4313	0.4199	0.4426	0.4313
(iii)	0.4109	0.4489	0.4299	0.4110	0.4489	0.4300
(iv)	0.4533	0.4121	0.4327	0.4128	0.4527	0.4328
(v)	0.4566	0.4136	0.4351	0.4136	0.4566	0.4351
(vi)	0.4292	0.4283	0.4289	0.4285	0.4291	0.4288
(vii)	0.4406	0.4168	0.4287	0.4168	0.4406	0.4287
(viii)	0.4067	0.4451	0.4259	0.4066	0.4451	0.4259
(ix)	0.4512	0.4096	0.4304	0.4097	0.4511	0.4304
(x)	0.4546	0.4111	0.4329	0.4105	0.4501	0.4303

4.3.2. Spin Density Distribution

Hund's rule based spin alternation rule,[73,74] is very helpful to predict the ground state magnetism for diradicals coupled with different couplers. This rule states that when the pathway through the coupler propagates through an even number of bonds, ferromagnetism arises. Kiovisto and Hicks[7] have discussed the fact that bis-oxoverdazyl diradical possess a

plane of symmetry through the linkage bond between two monoradicals, as a result, the spin distribution is subdued and antiferromagnetism arises. However, the linkage position of the π-donor unit to an aromatic ring coupler determines the sign of J. It is widely recognized that *meta*-phenylene coupled diradicals exhibit a high ferromagnetically signed interaction.[9,10,31-34] In our present chapter, we have used "*meta*"-coupled linear polyacene spacers of varying length between two oxo-verdazyl and two thio-verdazyl monoradicals and found that all the diradicals strictly follow the spin alternation rule (Figure 4.2). Indeed, the consequences of

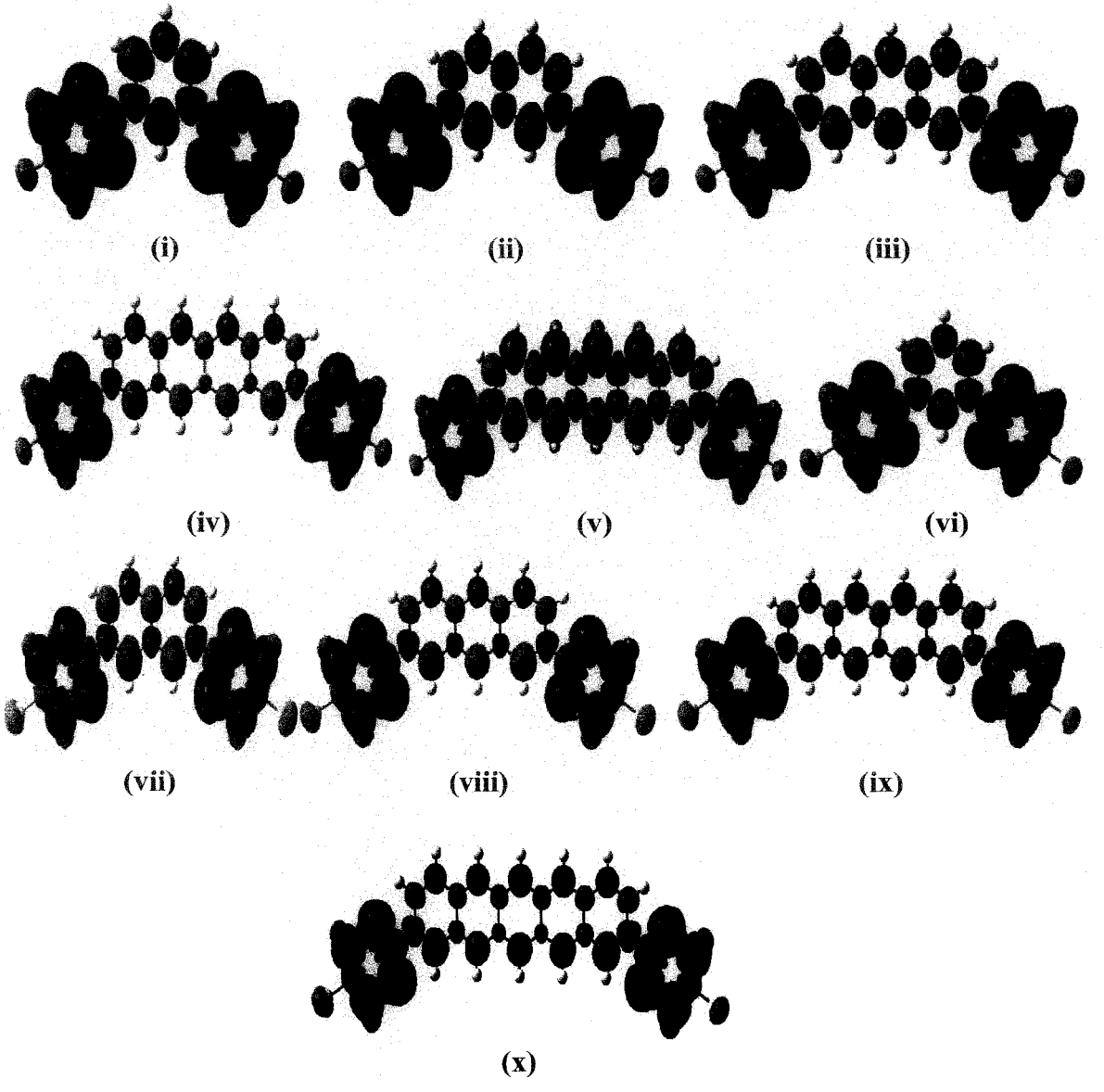

Figure 4.2. Spin-density distribution plots for each of the diradicals (i–x); blue color indicates α spin, and green color indicates β spin respectively.

this spin-alternation rule follows directly from the results[76-78] for alternant conjugated π-networks that the total ground-state spin is half of the difference between the number of spins on "starred" and "unstarred" sites. An alternant network is such that the sites can be partitioned into the starred and unstarred sites with every neighboring pair of sites of different types. That is, in a diradical species, the two unpaired electrons are, predicted to give a "triplet" or a "singlet" ground state as the two electrons are respectively on like (i.e., both "starred" and both "unstarred") or unlike (i.e., one is "starred" and the other "unstarred"). It is also to be noted that two like sites are separated by an even number of bonds, while unlike sites are separated by odd number of bonds, which is essentially the same as that given by Trindle et al.[73,74] This general result arises in the context of the nearest neighbor Heisenberg spin model, which is equivalent to the covalent-space Pauling-Wheland VB model. This theorematic result is a consequence of a general symmetry feature of the no des of the many-electron wave-function.[76] However, these theorematic results apply when the average formal number of π-electrons per site in the π-network is 1.[79] If one includes in the π-network a different number of π-electrons, that is, when one introduces a formally neutral N atom with 3 σ-bonds and a net contribution of 2 π-electrons, then a different situation arises. To understand this, when two N atoms are neighbors, as that in verdazyl, with one N atom formally contributing 1 π-electron and the other 2, there is a major ground-state contribution with spin$\uparrow$ on the first site and spin$\uparrow\downarrow$ on the second site. This configuration also interacts with another configuration via electron transfer, with spin$\uparrow\downarrow$ on the first site and spin$\uparrow$ on the second site. Thus one finds parallel spins on these two neighboring N-atom sites which are in agreement with our computational results, as illustrated in Figure 4.2.

4.3.3. Analysis of Singly Occupied Molecular Orbitals (SOMOs)

With the help of extended Hückel theory (ETH), Hoffmann[80] suggested that if the energy difference is less than 1.5 eV between two consecutive SOMOs, then parallel orientation of spins occurs. However, the theorem concerning the number of sites of the two different types ("starred" and "unstarred"), indicates the situation which is generally more nuanced. Within the MO framework, one also needs to figure out the overlap between the

SOMOs, for which the argumentation leading to Hund's rule is severely weakened.[16,81] At the B3LYP level with 6-31G(d,p) basis set, $4n\pi$ anti-aromatic linear and angular polyheteroacenes have been investigated by Constantinides et al.;[82] where they found that for a SOMO splitting ΔE_{SS}>1.3 eV, a singlet ground state results with antiparallel orientation of spins. The critical value of ΔE_{SS} is different in different cases.[34] In this chapter, we calculate the SOMO-SOMO energy gap for the "triplet" ground state of all 10 diradicals. It is observed that, diradicals (i) in set A and (vi) in set B have the lowest ΔE_{SS} (Table 4.4) value with the highest J value in their respective sets. Among the diradicals (i), (ii), (iii) (in set A) and (vi), (vii), (viii) (in set B) the ΔE_{SS} value increases as the J value decreases. This observation makes it clear that our calculations are consistent with the Hay-Thibeault-Hoffmann[83] (HTH) formula for the singlet-triplet energy gap in weakly coupled dinuclear metal complexes.

Table 4.4. The energy of SOMOs in *au* and their differences in eV at UB3LYP level using a 6-31G(d, p) basis set for diradicals (i-x).

Diradicals	$E_S(1)au$	$E_S(2)au$	$\Delta E_{SS}eV$
(i)	–0.20778	–0.20771	0.0019
(ii)	–0.20774	–0.20681	0.0253
(iii)	–0.20744	–0.19874	0.2367
(iv)	–0.20706	–0.18565	0.5826
(v)	–0.20665	–0.17576	0.8406
(vi)	–0.21952	–0.21941	0.0030
(vii)	–0.21878	–0.21739	0.0378
(viii)	–0.21778	–0.20625	0.3137
(ix)	–0.21698	–0.19244	0.6678
(x)	–0.21587	–0.18212	0.9184

However, for last two diradicals in each set, the ΔE_{SS} values are higher; despite they show high values of J. This is due to the fact that larger polyacenes possess within themselves a significant radicaloid character, with a "triplet" state approaching toward the singlet ground state, which then may be better viewed as an open-shell singlet. This observation is also found in recent computations,[35,84,85] but this is also conceivable from reasonable extensions of "classical" arguments of Clar.[86] If one imagines that as the length of an N-acene increases, the N+1 ordinary single Clar-sextet structures become of ever lesser importance

than the diradicaloid two-Clar-sextet structures, for which there is a much greater number $=\frac{1}{12}N(N-1)^2(N-2)$. In fact, Clar paid little attention to radicals, though recent extensions[87,88] to deal with radicaloid species reflect favorably on his ideas, and such natural extensions follow. The point is that with an extended diradicaloid nature for the spacer, its spin-polarization is eased, and the communication (as mediated by J) is enhanced. In any event in this present chapter, all 10 diradicals under investigation have ΔE_{SS}<1.5 eV and show manifestly ferromagnetic coupling. Thus, even if it is not conclusively proved that the Kohn-Sham orbital energies have a relationship with the magnetic coupling constants, this analysis provides justification of such a connection, albeit empirically.

4.3.4. Nuclear Independent Chemical Shift (NICS)

The quintessence of aromaticity can be straightforwardly documented with ease, yet it is

Table 4.5. The calculated NICS values at the centre of the aromatic rings at UB3LYP level using a 6-311+G(d, p) basis set for diradicals (i-x).

Diradical	NICS	A	B	C	D	E
(i)	NICS(0)	–6.62				
	NICS(1)	–8.96				
(ii)	NICS(0)	–8.77	–8.77			
	NICS(1)	–9.46	–9.46			
(iii)	NICS(0)	–6.62	–9.90	–6.62		
	NICS(1)	–8.81	–11.71	–8.81		
(iv)	NICS(0)	–5.81	–10.25	–10.24	–5.80	
	NICS(1)	–8.12	–11.95	–11.95	–8.11	
(v)	NICS(0)	–5.10	–9.64	–11.20	–9.64	–5.10
	NICS(1)	–7.49	–1.43	–12.65	–11.43	–7.49
(vi)	NICS(0)	–6.56				
	NICS(1)	–8.99				
(vii)	NICS(0)	–7.21	–7.27			
	NICS(1)	–9.55	–9.51			
(viii)	NICS(0)	–6.42	–10.00	–6.29		
	NICS(1)	–8.87	–11.80	–8.82		
(ix)	NICS(0)	–5.63	–10.25	–10.25	–5.75	
	NICS(1)	–8.14	–11.99	–11.99	–8.18	
(x)	NICS(0)	–4.88	–9.60	–11.24	–9.63	–5.02
	NICS(1)	–7.50	–1.46	–12.70	–11.45	–7.55

tricky to categorize quantitatively because of its multidimensional[89-92] or partially-ordered[93,94] nature. In some interesting work, Illas and co-workers[95] and Feixas et al.[96] have shown that different measures of aromaticity exhibit some discrepancies. There are many descriptors to study aromaticity, but NICS, which is a local aromaticity index, has many advantages over others. The NICS values depend on the methodology used and the basis set employed.[90-92] In our present chapter, the NICS values for all aromatic rings in 10 different diradicals are calculated by using GIAO-UB3LYP methodology with a 6-311+G(d,p) basis set. The NICS values are calculated at the centre of the ring [NICS (0)] and 1Å above the ring surface [NICS (1)], where, π-orbital density is maximum. Schleyer and coworkers[90-92]

Table 4.6. The calculated NICS(1) values for the all the diradicals (i-x) and corresponding acene molecules, ΔNICS(1), at UB3LYP level using 6-311+G(d,p) basis set, where (*) sign represents the NICS(1) values in bis-oxo- and bis-thioxo-verdazyl diradicals (Table 4.5), on the other hand, (**) sign represents the NICS(1) values in acene molecules without bis-oxo- and bis-thioxo-verdazyl diradicals as given in ref. 92.

	Average NICS(1)		
Diradicals	Couplers*	Acenes**	ΔNICS(1)
(i)	–8.96	–10.60	1.64
(ii)	–9.46	–10.80	1.34
(iii)	–9.78	–11.00	1.22
(iv)	–10.03	–11.10	1.07
(v)	–10.10	–11.20	1.10
(vi)	–8.99	–10.60	1.61
(vii)	–9.53	–10.80	1.27
(viii)	–9.83	–11.00	1.17
(ix)	–10.08	–11.10	1.02
(x)	–10.13	–11.20	1.07

have studied linear polyacene molecules with B3LYP/6-311+G(d,p) level using GIAO-B3LYP methodology. Ali and Datta[10] also have used the same methodology and basis sets for nitronyl nitroxide based polyacene spacers. These authors have noticed that terminal rings in the linear polyacenes have less benzenoid character and the inner rings are more aromatic

than benzene itself. These results are in good agreement with the results obtained in this chapter (Table 4.5). It is observed from Table 4.6 that $NICS(1)_{coupler} < NICS(1)_{acenes}$. The difference between average $NICS(1)_{coupler}$ and $NICS(1)_{acene}$ is represented by ΔNICS(1). For both set of diradicals it is obvious that the average NICS(1) value per benzenoid ring increases as the size of the coupler increases. It is also observed that with the decrease of ΔNICS(1), J value decreases for the first three species in each set but the reverse trend is observed for the last two species in both sets of diradicals due to the increase of diradical character of the couplers as discussed in the previous section.

4.3.5. Isotropic Hyperfine Coupling Constants (HFCCs)

Isotropic hyperfine coupling constant (HFCC), the interaction between nuclear and electric magnetic moments depends on the spin density of the related nuclei. HFCCs are difficult to calculate because of electron correlation and basis-set effects. Solvent also often plays an effective role to influence the HFCC values. In our present chapter, we have calculated HFCCs within the DFT framework by using an EPR-II basis set at the UB3LYP level in vacuum. As it turns out, "S" atoms are not considered in the EPR-II basis set in the quantum chemical package used for computations[69] so we have used the 6-31G(d,p) basis set for "S" atoms in all set B diradicals.

In oxo-vardazyl and thioxo-verdazyl monoradicals, two sets of two equivalent nitrogen atoms (N_1-N_5 and N_2-N_4) (Scheme 4.1) are found. Plater et al.[97] in bis-verdazyl diradical have observed that hfcc for $a(N_2\text{-}N_4)$ = 6.5 G and $a(N_1\text{-}N_5)$ = 5.3 G (depending upon the nature of substitution), which are nearly similar to that observed by Neugebauer et al.[27,98] They have also found that larger hfcc values are obtained at N_2, N_4 and N_{10}, N_{14} which means that the spins are localized along the N=C–N group rather than over the Me–N–CO–N–Me group (Scheme 4.1). Nitronyl nitroxide diradical with different couplers[9,10] have been studied and the HFCC values for conjugated coupler added diradicals reduce to half of the values for corresponding monoradicals.

In our present chapter, we have computed HFCC values for all eight N-atoms present in each bis-oxo- and thioxo-verdazyl diradical (Table 4.7). From these computations we see that the calculated gas phase HFCC values for N_2-N_4 and N_{10}-N_{14} are larger than that of N_1-N_5 and N_{11}-N_{13} (Scheme 4.1) in both sets of diradicals. These results are in good agreement with many experiments.[27,98] However, we do not find a clear relationship between the HFCC values and the exchange-coupling constants.

Table 4.7. Evaluated hyperfine coupling constant (HFCC) in *Gauss* at UB3LYP level using EPR- II basis set [for "S" atom 6-31G(d,p) basis set is employed] for all diradicals.

Diradicals	a_{N1}	a_{N2}	a_{N4}	a_{N5}	a_{N10}	a_{N11}	a_{N13}	a_{N14}
(i)	1.39456	2.81214	2.81926	1.38991	2.80826	1.38999	1.39465	2.82350
(ii)	1.37680	2.84858	2.50333	1.32396	2.84127	1.38191	1.31987	2.51208
(iii)	1.21091	2.19120	2.97822	1.34377	2.75415	1.33215	1.40500	3.10998
(iv)	1.28194	2.71955	2.13397	1.17365	2.72345	1.29045	1.18250	2.16933
(v)	1.41566	3.14904	2.57570	1.30419	3.14903	1.41564	1.30422	2.57576
(vi)	1.18701	3.17927	3.26141	1.12447	3.17827	1.18679	1.12477	3.26315
(vii)	1.49530	3.19138	3.03626	1.14349	3.19407	1.46392	1.36941	3.04159
(viii)	1.88941	2.93919	3.15984	1.71353	2.94157	1.89106	1.70922	3.15784
(ix)	1.44644	3.32940	3.60754	1.83785	3.16914	1.77647	1.76401	2.87529
(x)	1.33400	3.01129	2.74187	1.27111	3.01187	1.03849	1.23550	2.73678

4.4. Conclusions

This chapter presents a theoretical study of magnetic intramolecular coupling in bis-oxoverdazyl and bis-thioxoverdazyl diradicals with polyacene spacers using a density functional theory based method within the broken symmetry approach to estimate the energy of the open shell singlet. We discuss the results in light of correlation with several qualities related to spin density. This subject is of interest for the community seeking for stable organic ferromagnets. Although we have used the unrestricted B3LYP exchange-correlation potential, recent advances have shown that other functionals, such as functionals of M06 family[99] and the range-separated functionals[100] represent a considerable improvement over B3LYP. Bis-verdazyl is one of the compounds included to study the usefulness of such

functionals; thus, these functionals are promising to study organic ferromagnets. In our study, all 10 diradicals (i)-(x), have been found to be ferromagnetic in nature (i.e., with a "triplet" ground state). A general site-type-classification given by theorematically based rule,[76,77] accurately predicts the sign of J, as well as the spin-density alternation pattern,[78] which is also consonant with an empirically designed rule[73,74] for the sign of J. The exchange-coupling interactions are mainly transmitted through conjugated π-electron network as observed by other authors.[9,10,31-34] It is emphasized that this coupling between distant diradical sites is enhanced when the coupler itself has a low-lying excited "triplet" state with spin-density spread over the intervening space, as manifested in (iv), (v) and (ix), (x). A clear signature of this effective transmission is seen in the strong spin-density alternation (Figure 4.2) pattern, as obvious from an MO analysis. The J values decrease (Table 4.1) from X=1 to X=3 (Scheme 4.1) but increase from X=3 to X=5 for both sets of diradicals. The increase in J value in the later case is due to the evident increase of diradical character of tetracene and pentacene couplers. In dimetal systems which exhibit little charge transfer from ligands to metals, predicted J values are found to be pretty accurate.[101] In the present study, our systems do not seem to be susceptible to much charge transfer onto the spin centers. Thereby, we expect that the predicted J values should be accurate in analogy with the inorganic complexes. However, this generalization needs systematic study with organic systems. To compare our results with experimental works, we find Gilroy et al.[31] have reported 1,3-benzene-bridged *N,N'*-di(isopropyl)-6-oxoverdazyl diradical from empirical method by measuring magnetic susceptibility data at different temperatures. They have found that the diradical has a high-spin ground state with J =19.3 ± 1.7 cm^{-1}. In our DFT study, we get J = 67 cm^{-1} (Table 4.1), at the optimized level for diradical (i) which is essentially a similar diradical studied by Gilroy et al.,[31] with only difference is that the isopropyl groups are substituted by the hydrogens. Thus, our results are in good agreement with experimental work. In case of bis-thioxo-verdazyl series not many experimental studies are reported. Nevertheless, from this study it is clear that bis-thioxo verdazyls are good precursors for single molecule magnets. In this study, we notice that the J values are found to increase with bond order between the coupler and the radical fragments, which is manifested in spin population analysis. The NICS values (Table 4.5) are higher for the central benzenoid ring(s) of each coupler, while it is found that terminal rings have low NICS values, that is, a loss of

benzenoid character is observed.[90-92] However, for tetracene and pentacene coupled diradicals in both sets, the J value increases due to increase in open-shell radicaloid character of the spacers. Finally, this chapter also estimates HFCC values.

This work has been published in Theoretical Chemistry Accounts (Ref. 102).

4.5. References and Notes

(1) Kahn, O. *Molecular Magnetism*, New York, VCH, 1993.

(2) Coronado, E.; Delhaè, P.; Gatteschi, D.; Miller, J. S. *Molecular Magnetism: From Molecular Assemblies to the Devices*, Eds.; Nato ASI Series E, Applied Sciences, Kluwer Academic Publisher: Dordrecht, Netherland, 1996, Vol. 321.

(3) Benelli, C.; Gatteschi, D. *Chem. Rev.* **2002**, *102*, 2369.

(4) Tamura, M.; Nakazawa, Y.; Shiomi, D.; Nozawa, K.; Hosokoshi, Y.; Ishikawa, M.; Takahashi, M.; Kinoshita, M. *Chem. Phys. Lett.* **1991**, *186*, 401.

(5) Dougherty, D. A. *Acc. Chem. Res.* **1991**, *24*, 88.

(6) Borden, W. T.; Iwamura, H.; Berson, J. A. *Acc. Chem. Res.* **1994**, *27*, 109.

(7) Koivisto, B. D.; Hicks, R. G. *Coord. Chem. Rev.* **2005**, *249*, 2612.

(8) Ziessel, R.; Stroh, C.; Heise, H.; Khler, F. H.; Turek, P.; Claiser, N.; Souhassou, M.; Lecomte, C. *J. Am. Chem. Soc.* **2004**, *126*, 12604.

(9) Ali, Md. E.; Datta, S. N. *J. Phys. Chem. A* **2006**, *110*, 2776.

(10) Ali, Md. E.; Datta, S. N. *J. Phys. Chem. A* **2006**, *110*, 13232.

(11) Takeda, K.; Hamano, T.; Kawae, T.; Hidaka, M.; Takahash, M.; Kawasaki, S.; Mukai, K. *J. Phys. Soc. Jpn.* **1995**, *64*, 2343.

(12) Mukai, K.; Konishi, K.; Nedachi, K.; Takeda, K. *J. Phys. Chem.* **1996**, *100*, 9658.

(13) Kuhn, R.; Trischmann, H. *Angew. Chem. Int. Ed. Engl.* **1963**, *2*, 155.

(14) Fico, R. M. Jr.; Hay, M. F.; Reese, S.; Hammond, S.; Lambert, E.; Fox, M. A. *J. Org. Chem.* **1999**, *64*, 9386.

(15) Brook, D. J. R.; Fox, H. H.; Lynch, V.; Fox, M. A. *J. Phys. Chem.* **1996**, *100*, 2066.

(16) Borden, W. T.; Davidson, E. R. *J. Am. Chem. Soc.* **1977**, *99*, 4587.

(17) Neugebauer, F. A.; Fischer, H.; Krieger, C. *J. Chem. Soc. Perkin. Trans.* **1993**, *2*, 535.

(18) Mukai, K.; Konishi, K.; Nedachi, K.; Takeda, K. *J. Magn. Magn. Mater.* **1995**, *140*, 1449.

(19) Mukai, K.; Nedachi, K.; Takiguchi, M.; Kobayashi, T.; Amaya, K. *Chem. Phys. Lett.* **1995**, *238*, 61.

(20) Kremer, R. K.; Kanellakopulos, B.; Bele, P.; Brunner, H.; Neugebauer, F. A. *Chem. Phys. Lett.* **1994**, *230*, 255.

(21) Mito, M.; Nakano, H.; Kawae, T.; Hitaka, M.; Takagi, S.; Deguchi, H.; Suzuki, K.; Mukai, K.; Takeda, K. *J. Phys. Soc. Jpn.* **1997**, *66*, 2147.

(22) Mukai, K.; Nuwa, M.; Morishita, T.; Muramatsu, T.; Kobayashi, T. C.; Amaya, K. *Chem. Phys. Lett.* **1997**, *272*, 501.

(23) Jamali, J. B.; Achiwa, N.; Mukai, K.; Suzuki, K.; Ajiro, Y.; Matsuda, K.; Iwamura, H. *J. Magn. Magn. Mater.* **1998**, *177*, 789.

(24) Mukai, K.; Wada, N.; Jamali, J. B.; Achiwa, N.; Narumi, Y.; Kindo, K.; Kobayashi, T.; Amaya, K. *Chem. Phys. Lett.* **1996**, *257*, 538.

(25) Jamali, J. B.; Wada, N.; Shimobe, Y.; Achiwa, N.; Kuwajima, S.; Soejima, Y.; Mukai, K. *Chem. Phys. Lett.* **1998**, *292*, 661.

(26) Hamamoto, T.; Narumi, Y.; Kindo, K.; Mukai, K.; Shimobe, Y.; Kobayashi, T. C.; Muramatsu, T.; Amaya, K. *Physica B* **1998**, *246*, 36.

(27) Neugebauer, F. A.; Fischer, H.; Siegel, R. *Chem. Ber.* **1988**, *121*, 815.

(28) Serwinski, P. R.; Esat, B.; Lahti, P. M.; Liao, Y.; Walton, R.; Lan, J. *J. Org. Chem.* **2004**, *69*, 5247.

(29) Hicks, R. G.; Koivisto, B. D.; Lemaire, M. T. *Org. Lett.* **2004**, *12*, 1887.

(30) Hicks, R. G.; Hooper, R. *Inorg. Chem.* **1999**, *38*, 284.

(31) Gilroy, J. B.; McKinnon, S. D. J.; Kennepohl, P.; Zsombor, M. S.; Ferguson, M. J.; Thompson, L. K.; Hicks, R. G. *J. Org. Chem.* **2007**, *72*, 8062.

(32) Polo, V.; Alberola, A.; Andres, J.; Anthony, J.; Pilkington, M. *Phys. Chem. Chem. Phys.* **2008**, *10*, 857.

(33) Latif, I. A.; Panda A.; Datta S. N. *J. Phys. Chem. A* **2009**, *113*, 1595.

(34) Bhattacharya, D.; Misra, A. *Phys. Chem. A* **2009**, *113*, 5470.

(35) Bendikov, M.; Duong, H. M.; Starkey, K.; Houk, K. N.; Carter, E. A.; Wudl, F. *J. Am. Chem. Soc.* **2004**, *126*, 7416.

(36) Clar, E. *Polycyclic Hydrocarbons*, Academic Press: London, 1964, Vols. 1, 2.

(37) Hegmann, F. A.; Tykwinski, R. R.; Lui, K. P. H.; Bullock, J. E.; Anthony, J. E. *Phys. Rev. Lett.* **2002**, *89*, 227403.

(38) Houk, K. N.; Lee, P. S.; Nendel, M. *J. Org. Chem.* **2001**, *66*, 5517.

(39) Chung, G.; Lee, D. *Chem. Phys. Lett.* **2001**, *350*, 339.

(40) de Graaf, C.; Sousa, C.; Moreira, I. de P. R.; Illas, F. *J. Phys. Chem. A* **2001**, *105*, 11371.

(41) Noodleman, L. *J. Chem. Phys.* **1981**, *74*, 5737.

(42) Noodleman, L.; Baerends, E. J. *J. Am. Chem. Soc.* **1984**, 106, 2316.

(43) Ginsberg A. P. *J. Am. Chem. Soc.* **1980**, *102*, 111.

(44) Noodleman, L.; Peng, C. Y.; Case, D. A.; Mouesca, J.-M. *Coord. Chem. Rev.* **1995**, *144*, 199.

(45) Noodleman, L.; Davidson, E. R. *Chem. Phys.* **1986**, *109*, 131.

(46) Bencini, A.; Totti, F.; Daul, C. A.; Doclo, K.; Fantucci, P.; Barone, V. *Inorg. Chem.* **1997**, *36*, 5022.

(47) Bencini, A.; Gatteschi, D.; Totti, F.; Sanz, D. N.; McClevrty, J. A.; Ward, M. D. *J. Phys.Chem. A* **1998**, *102*, 10545.

(48) Ruiz, E.; Cano, J.; Alvarez, S.; Alemany, P. *J. Comput. Chem.* **1999**, *20*, 1391.

(49) Caballol, R.; Castell, O.; Illas, F.; Moreira, I. de P. R.; Malrieu, J. P. *J. Phys. Chem. A* **1997**, *101*, 7860.

(50) Moreira, I. de P. R.; Illas, F. *Phys. Chem. Chem. Phys.* **2006**, *8*, 1645.

(51) Illas, F.; Moreira, I. de P. R.; Bofill, J. M.; Filatov, M. *Phys. Rev. B* **2004**, *70*, 132414.

(52) Moreira, I. de P. R.; Costa, R.; Filatov, M.; Illas, F. *J. Chem. Theor. Comput.* **2007**, *3*, 764.

(53) Illas, F.; Moreira, I. de P. R.; Bofill J. M.; Filatov M. *Theor. Chem. Acc.* **2006**, *116*, 587.

(54) Yamaguchi, K.; Takahara, Y.; Fueno, T.; Nasu, K. *Jpn. J. Appl. Phys* **1987**, *26*, L1362.

(55) Yamaguchi, K; Tsunekawa, T.; Toyoda, Y.; Fueno, T. *Chem. Phys. Lett.* **1988**, *143*, 371.

(56) Yamaguchi, K.; Jensen, F.; Dorigo, A.; Houk, K. N. *Chem. Phys. Lett.* **1988**, *149*, 537.

(57) Yamaguchi, K.; Takahara, Y.; Fueno, T.; Houk, K. N. *Theor. Chim. Acta.* **1988**, *73*, 337.

(58) Ruiz, E.; Alvarez, S.; Cano, J.; Polo, V. *J. Chem. Phys.* **2005**, *123*, 164110.

(59) Adamo, C.; Barone, V.; Bencini, A.; Broer, R.; Filatov, M.; Harrison, N. M.; Illas, F.; Malrieu, J. P.; Moreira, I. de P. R. *J. Chem. Phys.* **2006**, *124*, 107101.

(60) Polo, V.; Gräfenstein, J.; Kraka, E.; Cremer, D. *Theor. Chem. Acc.* **2003**, *109*, 22.

(61) Gräfenstein, J.; Kraka, E.; Filatov, M.; Cremer, D. *Int. J. Mol. Sci.* **2002**, *3*, 360.

(62) Martin, R. L.; Illas, F. *Phys. Rev. Lett.* **1997**, *79*, 1539.

(63) Becke, A. D. *Phys. Rev. A* **1988**, *38*, 3098.

(64) Lee, C. T.; Yang, W. T.; Parr, R. G. *Phys. Rev. B* **1988**, *37*, 785.

(65) Becke, A. D. *J. Chem. Phys.* **1993**, *98*, 5648.

(66) Hehre, W. J.; Ditchfield, R.; Pople, J. A. *J. Chem. Phys.* **1972**, *56*, 2257.

(67) Hariharan, P. C.; Pople, J. A. *Theor. Chim. Acta* **1973**, *28*, 213.

(68) Francl, M. M.; Pietro, W. J.; Hehre, W. J.; Binkley, J. S.; Gordon, M. S.; Defrees, D. J.; Pople, J. A. *J. Chem. Phys.* **1982**, *77*, 3654.

(69) Frisch, M. J.; Trucks, G. W.; Schlegel, H. B.; Scuseria, G. E.; Robb, M. A.; Cheeseman, J. R.; Montgomery, J. A. Jr.; Vreven, T.; Kudin, K. N.; Burant, J. C.; Millam, J. M.; Iyengar, S. S.; Tomasi, J. J.; Barone, V.; Mennucci, B.; Cossi, M.; Scalmani, G.; Rega, N.; Petersson, G. A.; Nakatsuji, H.; Hada, M.; Ehara, M.; Toyota, K.; Fukuda, R.; Hasegawa, J ; Ishida, M.; Nakajima, T.; Honda, Y.; Kitao, O.; Nakai, H.; Klene, M.; Li, X.; Knox, J. E.; Hratchian, H. P.; Cross, J. B.; Bakken, V.; Adamo, C.; Jaramillo, J.; Gomperts, R.; Stratmann, R. E.; Yazyev, O.; Austin, A. J.; Cammi, R.; Pomelli, C.; Ochterski, J.; Ayala, P. Y.; Morokuma, K.; Voth, A.; Salvador, P.; Dannenberg, J. J.; Zakrzewski, V. G.; Dapprich, S.; Daniels, A. D.; Strain, M. C.; Farkas, O.; Malick, D. K.; Rabuck, A. D.; Raghavachari, K.; Foresman, J. B.; Ortiz, J. V.; Cui, Q.; Baboul, A. G.; Clifford. S.; Cioslowski, J.; Stefanov, B. B.; Liu, G.; Liashenko, A.; Piskorz, P.; Komaromi, I.; Martin, R. L.; Fox, D. J.; Keith, T.; Al-Laham, M. A.; Peng, C. Y.; Nanayakkara, A.; Challacombe, M.; Gill, P. M. W.; Johnson, B.; Chen, W.; Wong, M. W.; Gonzalez, C.; Pople, J. A. GAUSSIAN 03W (Revision D.01), Gaussian, Inc.: Wallingford, CT, (2004).

(70) Hyperchem Professional Release 7.5 for Windows; Hypercube Inc., Gainesville, 2002.

(71) Flükiger, P.; Lüthi, H. P.; Portmann, S.; Weber, J. MOLEKEL 4.0, J. Swiss Center for Scientific Computing, Manno, Switzerland, 2000.

(72) Brook, D. J. R.; Yee, G. T. *J. Org. Chem.* **2006**, *71*, 4889.

(73) Trindle, C.; Datta, S. N. *Int. J. Quantum Chem.* **1996**, *57*, 781.

(74) Trindle, C.; Datta, S. N.; Mallik, B. *J. Am. Chem. Soc.* **1997**, *119*, 12947.

(75) Wiberg, K. B. *Tetrahedron* **1968**, *24*, 1083.

(76) Lieb, E. H.; Mattis, D. C. *J. Math. Phys.* **1962**, *3*, 749.

(77) Ovchinnikov, A. A. *Theor. Chim. Acta* **1978**, *47*, 297.

(78) Klein, D. J.; Nelin, C.; Alexander, S.; Matsen, F. A. *J. Chem. Phys.* **1982**, *77*, 3101.

(79) Klein, D. J.; Alexander, S. A. *In Graph Theory and Topology in Chemistry*; King, R. B., Rouvay, D. H., Eds.; Elsevier: Amsterdam, The Netherlands, 1987; vol. 51, p 404. (80) Hoffmann, R.; Zeiss, G. D.; Van Dine, G. W. *J. Am. Chem. Soc.* **1968**, *90*, 1485.

(81) Borden, W. T.; Davidson, E. R. *Acc. Chem. Res.* **1981**, *14*, 69.

(82) Constantinides, C. P.; Koutentis, P. A.; Schatz, J. *J. Am. Chem. Soc.* **2004**, *126*, 16232.

(83) Hay, P. J.; Thibeault, C. J.; Hoffmann, R. *J. Am. Chem. Soc.* **1975**, *97*, 4884.

(84) Malloci, G.; Mulas, G.; Cappellini, G.; Joblin, C. *Chem. Phys.* **2007**, *340*, 43.

(85) Reddy, A. R.; Fridman-Marueli, G.; Benidikov, M. *J. Org. Chem.* **2007**, *72*, 51.

(86) Clar, E. *The Aromatic Sextet*, John Wiley and Sons, New York, 1970.

(87) Misra, A.; Klein, D. J.; Morikawa, T. *J. Phys. Chem. A* **2009**, *113*, 1151.

(88) Misra, A.; Schmalz, T. G.; Klein, D. J. *J. Chem. Inf. Model.* **2009**, *49*, 2670.

(89) Katrizky, A.; Barczymski, P.; Musumarra, G.; Pisano, D.; Szafran, M. *J. Am. Chem. Soc.* **1989**, *111*, 7.

(90) Schleyer, P. v. R.; Maerker, C.; Dransfeld, A.; Jiao, H.; Hommes, N. J. R. v. E. *J. Am. Chem. Soc.* **1996**, *118*, 6317.

(91) Schleyer, P. v. R.; Manoharan, M.; Jiao, H.; Stahl, F. *Org. Lett.* **2001**, *3*, 3643.

(92) Chen, Z.; Wannere, C. S.; Corminboeuf, C.; Puchta, R.; Schleyer, P. v. R. *Chem. Rev.* **2005**, *105*, 3842.

(93) Klein, D. J. *J. Chem. Edu.* **1992**, *69*, 691.

(94) Klein, D. J.; Babic, D. *J. Chem. Inf. Comp. Sci.* **1997**, *37*, 656.

(95) Poater, J.; García-Cruz, I.; Illas, F.; Solà, M. *Phys. Chem. Chem. Phys.* **2004**, *6*, 314.

(96) Feixas, F.; Matito, E.; Poater, J.; Solà, M. *J. Comp. Chem.* **2008**, *29*, 1543.

(97) Plater, M. J.; Kemp, S.; Coronado, E.; Gómez-García, C. J.; Harrington, R. W.; Clegg, W. *Polyhedron* **2006**, *25*, 2433.

(98) Neugebauer, F. A.; Fischer, H. *Angew. Chem. Int. Ed. Engl.* **1980**, *19*, 724.

(99) Valero, R.; Costa, R.; Moreira, I. de P. R.; Truhlar, D. G.; Illas, F. *J. Chem. Phys.* **2008**, *128*, 114103.

(100) Rivero, P.; Moreira, I. de P. R.; Illas, F.; Scuseria, G. E. *J. Chem. Phys.* **2008**, *129*, 184110.

(101) Ali, Md. E.; Datta, S. N. *J. Mol. Struct. (THEOCHEM)* **2006**, *775*, 1.

(102) Bhattacharya, D.; Shil, S.; Misra, A.; Klein, D. J. *Theor. Chem. Acc.* **2010**, *127*, 57.